

Highly optimized CO₂ capture by inexpensive nanoporous covalent organic polymers and their amine composites

Hasmukh A. Patel and Cafer T. Yavuz*

Received 30th May 2015, Accepted 16th June 2015

DOI: 10.1039/c5fd00099h

Carbon dioxide (CO₂) storage and utilization requires effective capture strategies that limit energy penalties. Polyethylenimine (PEI)-impregnated covalent organic polymers (COPs) with a high CO₂ adsorption capacity are successfully prepared in this study. A low cost COP with a high specific surface area is suitable for PEI loading to achieve high CO₂ adsorption, and the optimal PEI loading is 36 wt%. Though the adsorbed amount of CO₂ on amine impregnated COPs slightly decreased with increasing adsorption temperature, CO₂/N₂ selectivity is significantly improved at higher temperatures. The adsorption of CO₂ on the sorbent is very fast, and a sorption equilibrium (10% wt) was achieved within 5 min at 313 K under the flow of simulated flue gas streams. The CO₂ capture efficiency of this sorbent is not affected under repetitive adsorption–desorption cycles. The highest CO₂ capture capacity of 75 mg g⁻¹ at 0.15 bar is achieved under dry CO₂ capture however it is enhanced to 100 mg g⁻¹ in the mixed gas flow containing humid 15% CO₂. Sorbents were found to be thermally stable up to at least 200 °C. TGA and FTIR studies confirmed the loading of PEIs on COPs. This sorbent with high and fast CO₂ sorption exhibits a very promising application in direct CO₂ capture from flue gas.

Introduction

The issue of global warming resulting from increased atmospheric concentrations of carbon dioxide (CO₂) is arguably the most important environmental challenge facing the world today.^{1,2} Effective strategies of CO₂ remediation have to include capture and utilization in close connection with each other. To begin such an endeavour, capturing of CO₂ generated by large point sources, such as fossil-fuel-fired power gasification plants, is essential.³

Liquid amine scrubbing technology (20% to 30% aqueous solutions of alkanolamines) has been commercialized industrially for decades and it is the most suitable for high volume flue gas streams among the CO₂ separation technologies in the present scenario.⁴ The major shortcoming of the aqueous amine systems is

Graduate School of EEWS, Korea Advanced Institute of Science and Technology (KAIST), Daejeon 305-701, Republic of Korea. E-mail: yavuz@kaist.ac.kr

the high amount of energy required for the regeneration step due to the chemisorptive mechanism, degradation of amines, corrosion of equipment, and sluggish adsorption–desorption kinetics. Nanoporous solid adsorbents have been proposed to counter these shortcomings associated with aqueous amine systems. Organic, inorganic and organic–inorganic hybrid porous materials with high surface areas are used for the sorption, purification, and storage of gases due to their plentiful quantities, composition, pore topology and morphology.⁵ Solid adsorbents—activated carbons, zeolites, mesoporous silica, metal–organic frameworks and nanoporous polymers—have been utilized for CO₂ separation.^{3,6–8} Although these sorbents show high CO₂ adsorption capacities (under pure, dry CO₂ feeds), most of them don't demonstrate selective separation of CO₂ from the mixed gas streams at warmer temperatures and under flue gas conditions.

Amines supported on porous materials are highly selective towards CO₂ by an effective chemisorptive mechanism and their capture capacity is preserved in the presence of moisture unlike the sorbents based on physisorption.^{9–11} Additionally, the disadvantages associated with the traditional amine scrubbing technique, *i.e.*, high-energy sorbent regeneration and corrosion, could easily be overcome if amines are immobilized on porous solid supports. Amine immobilization is usually carried out through either chemical or physical binding on various porous supporting materials.^{12,13} Since the chemically tethered aliphatic amines may not be able to withstand harsh reaction conditions and is thus an expensive route, a facile synthetic route involving physical impregnation of polyamines on porous supports could be an alternative, cost-effective technique for CO₂ capture technology.¹⁴

Most of the studies oriented towards physically immobilized polyamines used a mesoporous silica support because of the presence of hydroxyl groups on the surface (facilitates hydrogen bonding with amines) and large pore channels (hold a large amount of amines). Goepfert *et al.* showed polyethylenimine (PEI) loaded fumed silica and found a CO₂ uptake capacity of 206 mg g⁻¹ at 298 K and 1 bar.¹⁵ In fact, polyamine impregnated silicas are the materials which demonstrated a CO₂ capture capacity of up to 349 mg g⁻¹ at warmer sorption conditions under a humid atmosphere however very few reports studied the CO₂/N₂ selectivity for silica–polyamines hybrids.¹⁴ Furthermore, the synthesis of mesoporous silica requires costly surfactants and raw materials, leading to costly CO₂ capture technologies.

Here, we have developed a low cost nanoporous covalent organic polymer (COP) for loading polymeric amines and presented an optimized concentration of amines required for CO₂ uptake for this type of nanoporous COP support. CO₂ and N₂ sorption characteristics of an amine impregnated sorbent are also studied with their CO₂/N₂ selectivity trends. Apart from static sorption experiments, we have also demonstrated regeneration behaviour and CO₂ sorption under a continuous flow of humid CO₂ mixed gas stream at warmer temperatures to establish the sorbent's functioning in simulated flue gas conditions.

Experimental

Materials

Branched polyethylenimine ($M_w = 800$, PEI-800), branched polyethylenimine ($M_w = 25\,000$, PEI-25 000), melamine, terephthalaldehyde, dimethyl sulfoxide

(DMSO), acetone, tetrahydrofuran and methanol were obtained from Aldrich, USA and used as received.

Synthesis of covalent organic polymer-19 (COP-19)

A slightly modified procedure by Schwab *et al.* was used.¹⁶ Melamine (4.0 g, 0.032 mol) was dissolved in 150 mL dimethyl sulfoxide and terephthalaldehyde (6.44 g, 0.048 mol) was added after the complete dissolution of melamine. The solution was heated to 180 °C under vigorous stirring in a nitrogen environment for 3 days. The reaction was allowed to cool to room temperature, and the solid obtained was filtered, washed with dimethyl sulfoxide (20 mL, 3×), water (20 mL, 4×), acetone (20 mL, 3×), tetrahydrofuran (15 mL, 3×) and CH₂Cl₂ (15 mL, 3×). The resulting off-white solid was dried under vacuum at 150 °C for 10 h. Product: 7.2 g.

Synthesis of PEI impregnated COP-19

The calculated amount of PEI-800 or PEI-25 000 was dissolved in 10 mL of methanol. To this solution, COP-19 was dispersed and stirred for 24 h at room temperature. The dispersion was subjected for centrifugation to separate out precipitates and dried at 80 °C for 24 h under vacuum. The amount of PEI and COP-19 used for each impregnation is listed in Table 1 with sample designation.

Characterisation

FTIR spectra were obtained on KBr disks using a Perkin-Elmer FT-IR spectrometer. Thermogravimetric analysis (TGA) was performed using a NETZSCH-TG 209 F3 instrument by heating the samples up to 800 °C at 10 °C min⁻¹ under a N₂ atmosphere. Nitrogen adsorption isotherms were obtained with a Micromeritics Triflex accelerated surface area and porosimetry analyser at 77 K after the samples were degassed at 120 °C for 5 h under vacuum. The surface area of the samples was calculated using the Brunauer-Emmett-Teller (BET) method. Low-pressure CO₂ and N₂ adsorption-desorption isotherms were measured at 273 K and 298 K using a Micromeritics Triflex system. IAST calculations were carried out by fitting adsorption isotherms with a single-site Langmuir model or a dual-site Langmuir model. These models were fitted only on the basis of deriving the best fit with adjusted *r*² values exceeding 0.999. The Origin Pro v8.5 program has been used to calculate IAST selectivity.¹⁷ The CO₂ sorption used 15% CO₂, 3.8% H₂O, 81.2% He gas mixtures under flow conditions at 313 K up to 20 min. The gas mixture flow rate was 80 mL min⁻¹. The sorbent was loaded in a column and the concentration of inward and outward gas mixture was measured using GC-MS. The sorbent was degassed in He flow at 100 °C before analysis.

Table 1 Experimental composition used for synthesis of PEI impregnated samples

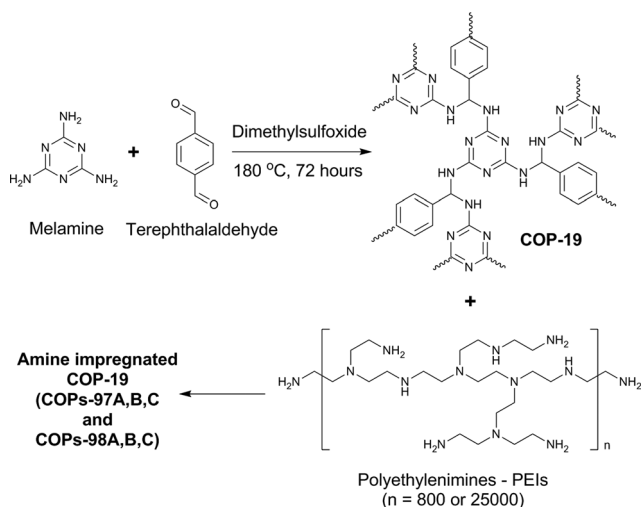
| Samples | COP-97A | COP-97B | COP-97C | COP-98A | COP-98B | COP-98C |
|------------|---------|---------|---------|---------|---------|---------|
| COP-19 | 0.25 g | 0.25 g | 0.25 g | 0.25 g | 0.25 g | 0.25 g |
| PEI-800 | 0.25 g | 0.5 g | 1.0 g | — | — | — |
| PEI-25 000 | — | — | — | 0.25 g | 0.5 g | 1.0 g |

Results and discussion

It is a prime requisite for CO₂ sorbents to be of minimal cost and this can only be possible if the sorbents can be produced using low cost raw materials and facile synthetic methodologies. Nanoporous COP-19 is synthesized through a one pot poly-condensation reaction of melamine and terephthalaldehyde (Scheme 1). COP-19 is utilized as a support for the immobilization of branched aliphatic amines of two different molecular weights (800 and 25 000 g mol⁻¹) and three different concentrations (Table 1), to demonstrate the effect of chain length and loading on the CO₂ uptake capacity. Thermogravimetric (TGA) and FTIR studies of COP-19 and amine impregnated COP-19 were carried out to obtain the amount of amine loaded on COP-19 and to show the structural stability of the support polymers.

The mass loss patterns of COP-19 and amine impregnated COP-19 were obtained from a TGA study under an inert atmosphere (Fig. 1a and b). The amount of amine loaded on COP-19 is calculated from the mass loss of amine impregnated COP-19 (COPs-97A,B,C and COPs-98A,B,C) normalized with the mass loss of COP-19. The calculated PEI-800 in COP-97A, COP-97B, and COP-97C is 24.1%, 36.4%, and 46.2% respectively while PEI-25 000 in COP-98A, COP-98B, and COP-98C is 22.4%, 32.3%, and 44.8% respectively. PEI-800 shows a slightly higher loading efficiency over PEI-25 000 because of the smaller steric size of the low molecular weight aliphatic amines. The TGA study also showed a thermal stability up to 200 °C for PEI impregnated COP-19.

FTIR spectra show evidence of amine impregnation and also demonstrate the stability of COP-19 after amine immobilization (Fig. 1c). The C–N stretching vibration is observed at 1150 cm⁻¹ and N–H stretching is clearly visible at 3500–3300 cm⁻¹, which is from merged peaks of primary and secondary amines. The broad peak and small intensity within this region is due to the presence of aliphatic amines. Broad peaks at 1640–1560 cm⁻¹ and 800 cm⁻¹ are due to a N–H



Scheme 1 Synthetic route for nanoporous COP-19 and PEI impregnation of COP-19.

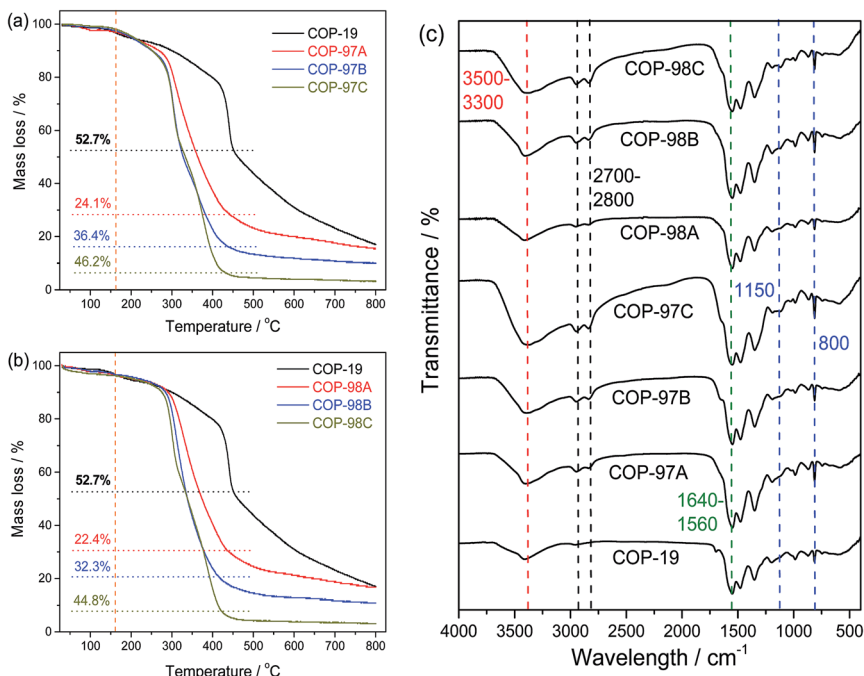


Fig. 1 (a and b) Thermogravimetric analysis of COP-19 and amine impregnated COP-19 up to 800 °C under a N₂ atmosphere. (c) FTIR spectra of COP-19 and amine impregnated COP-19 obtained as a KBr pellet.

in-plane-bend for primary amines. The vibration band at 2700–2800 cm⁻¹ is observed for C–H stretching of aliphatic chain of PEI and the intensity of this mode is higher than COP-19, clearly suggesting the presence of aliphatic amines.

The effect of amine impregnation on the porosity of the amine impregnated COP-19 is studied using N₂ adsorption–desorption isotherms at 77 K (Fig. 2). N₂ uptake at low relative pressure for COP-19 reveals the presence of micropores however it also shows a large uptake at higher relative pressure which is characteristic of meso–macro porous interconnected porosity in networked polymeric materials. COP-19 shows a Brunauer–Emmett–Teller (BET) surface area of 640 m² g⁻¹ which is substantially reduced after amine impregnation (Table 2). COP-97C and COP-98C (PEI loading ≈ 45% wt) became non-porous, mainly caused by blocking of accessible porosity of COP-19. The BET surface area of PEI supported COP-19 reduced upon an increase in amount of loading as well as the molecular chain length of the PEI. The BET surface area of COP-97A, COP-97B, COP-98A, and COP-98B is 118, 59, 88, and 47 m² g⁻¹ respectively. These results provide direction toward focusing on the linear low molecular weight aliphatic amines for a support material, which contain largely micro and meso porosity. It should also be noted that low molecular weight CO₂-philic amines may show lower thermal stability and thus degradation and loss of active species could be realised over a prolonged time.¹⁸

The moderate surface area and presence of CO₂-philic basic amine moieties on COP-19 are favourable to high CO₂ adsorption, particularly at very low pressure, a

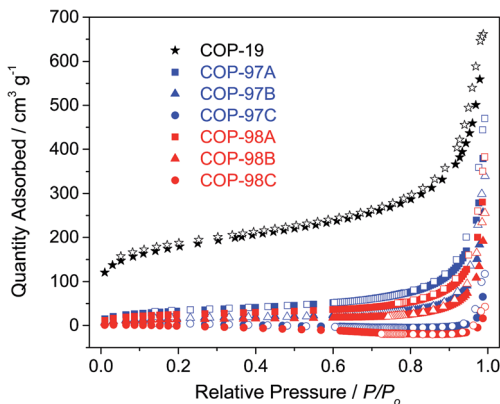


Fig. 2 N_2 adsorption–desorption isotherms of COP-19 and amine impregnated COP-19 at 77 K up to 1 bar. Filled and empty symbols correspond to adsorption and desorption respectively. The sorbents were activated at 120 °C under vacuum for 5 hours before each isotherm.

necessity for post-combustion CO_2 capture where the partial pressure of CO_2 ranges from 0.08–0.15 bar in flue gas streams. We studied CO_2 and N_2 sorption of COP-19 and amine impregnated COP-19 under static conditions at 273 and 298 K and up to 1 bar (Fig. 3 and Table 2).

Amine impregnated COP-19 (COP-97A,B,C and COP-98A,B,C) show very fast CO_2 uptake at low pressure compare to COP-19. PEI-800 loaded COP-97A, COP-97B, and COP-97C show a CO_2 uptake capacity of 95.5, 102.5 and 72 $mg\ g^{-1}$ at 273 K and 80.6, 96.7 and 62 $mg\ g^{-1}$ at 298 K, respectively at 1 bar. This suggests that PEI-800 loading of 24.1% wt is the optimum concentration for COP-19. Lower than this loading results in low capacity due to insufficient CO_2 -philic groups while higher loading causes pore blocking and thus restricts accessibility of the amines for CO_2 molecules. Furthermore, the formation of carbamate species upon reaction of CO_2 and amines also can block accessible CO_2 -philic sites.¹⁹ CO_2 isotherms at studied temperatures show fast CO_2 uptake for amine impregnated

Table 2 Surface area, CO_2 uptake and CO_2/N_2 selectivity of COP-19 and amine impregnated COP-19

| Sorbent | Surface area, $m^2\ g^{-1}$ | CO_2 uptake at 273 K, $mg\ g^{-1}$ | | CO_2 uptake at 298 K, $mg\ g^{-1}$ | | CO_2/N_2 selectivity | |
|---------|--------------------------------|---|-------|---|-------|---------------------------|--------|
| | | 0.15 bar | 1 bar | 0.15 bar | 1 bar | 273 K | 298 K |
| COP-19 | 640 | 45.4 | 107.4 | 17.7 | 58.3 | 141.5 | 131.2 |
| COP-97A | 118 | 63.6 | 95.5 | 50.6 | 80.6 | 574 | 965.6 |
| COP-97B | 59 | 75 | 102.5 | 69 | 96.7 | 445.3 | 779.2 |
| COP-97C | 7 | 47.5 | 72 | 37.6 | 62 | 1505 | 2511.4 |
| COP-98A | 88 | 70.4 | 115 | 53.3 | 99.2 | — | — |
| COP-98B | 47 | 63.2 | 95 | 58.2 | 90 | 452.6 | 852 |
| COP-98C | 2 | 43 | 68 | 38 | 63.6 | 813.7 | 1428 |

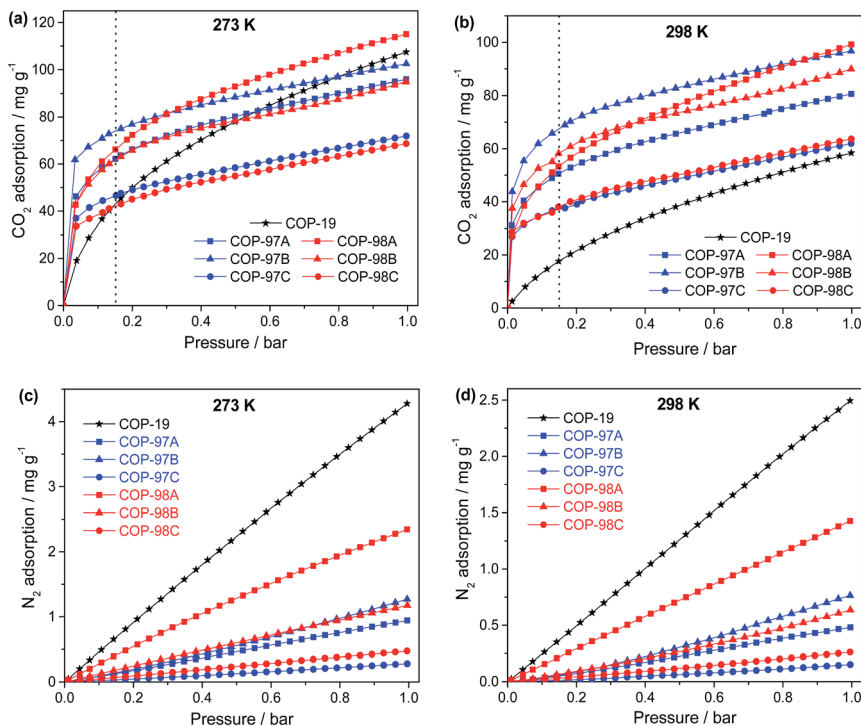


Fig. 3 CO_2 and N_2 adsorption isotherms of COP-19 and amine impregnated COP-19 at 273 K and 298 K up to 1 bar. The sorbents were activated at 120 °C under vacuum for 5 hours before each isotherm. Desorption profiles were omitted for clarity.

COP-19. The CO_2 sorption capacity at 0.15 bar for COP-97A, COP-97B, and COP-97C is 63.6, 75 and 47.5 mg g^{-1} at 273 K and 50.6, 69 and 37.6 mg g^{-1} at 298 K, respectively, however the CO_2 capture capacity of COP-19 is 45.4 and 17.7 mg g^{-1} at 273 and 298 K respectively. COP-97B demonstrated 1.65 and 3.9 times higher CO_2 uptake compare to COP-19 at 273 and 298 K. PEI-25 000 impregnated COP-98A, COP-98B and COP-98C also revealed similar trends of higher CO_2 uptake compare to COP-19 at 0.15 bar but lower than COP-97A,B,C (Fig. 3 and Table 2). N_2 sorption isotherms at 273 and 298 K show a decrease in the N_2 uptake with respect to an increase in the PEI loading. Owing to the non-reactivity of the N_2 molecule with amine functionality the N_2 sorption only depends on the availability of microporous porosity, which is filled and/or blocked by amines in impregnated samples. Indeed, lower N_2 sorption could be useful for attaining high CO_2 selective sorption from the mixture of gases.

CO_2/N_2 selectivity is one of the significant parameters for real applications of any sorbent material in CO_2 capture from flue gas streams, especially post-combustion CO_2 capture where N_2 concentration is as high as 85% in gas mixtures. Ideal adsorbed solution theory (IAST) is used in this study to illustrate CO_2/N_2 selectivity by a single-site Langmuir model or a dual-site Langmuir model fitting calculation of CO_2 and N_2 sorption isotherms.²⁰ CO_2/N_2 selectivity for CO_2 and N_2 (15 : 85) gas mixture against pressure is plotted in Fig. 4.

COP-19 shows CO_2/N_2 selectivity of 141.5 and 131.2 at 273 and 298 K respectively at 1 bar for a $\text{CO}_2 : \text{N}_2$ (15 : 85) mixture. A significant increase in CO_2/N_2 selectivity is observed for amine-impregnated samples, attributed to higher CO_2 uptake in CO_2 -philic PEI loaded sorbents. Although the CO_2 capture capacity of COP-97C is relatively low compared to COP-97B, it showed the highest CO_2/N_2 selectivity of 1505 and 2511.4 at 273 and 298 K. COP-97B demonstrated a CO_2/N_2 selectivity of 445.3 and 779.2 at 273 and 298 K. Other PEI impregnated samples also showed excellent CO_2/N_2 selectivity, ranging from 452.6–1428 at 273 and 298 K (Table 2). The increase in the CO_2/N_2 selectivity with increase in temperature is a significant characteristic since post-combustion CO_2 capture requires CO_2 sorption at high temperatures. A similar phenomenon can be observed for azo linked covalent organic polymers (azo-COPs) where the azo functionality was found to be N_2 -phobic.²¹ Here, however, the increment in selectivity at high temperatures resulted predominantly from CO_2 -philic functionalities. It is also noticeable that higher CO_2 capture and CO_2/N_2 selectivity is obtained in amine impregnated sorbents even though their surface area ranges from moderate to

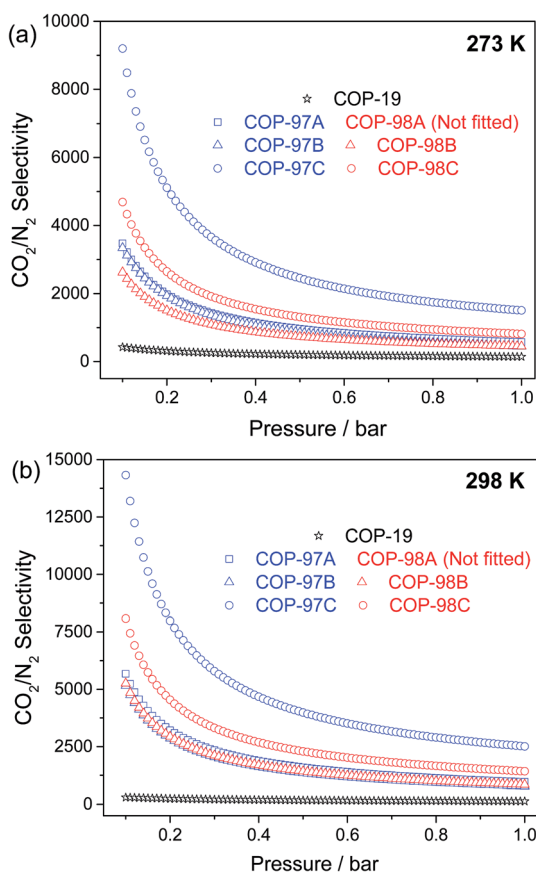


Fig. 4 IAST CO_2/N_2 selectivity of COP-19 and amine impregnated COP-19 at (a) 273 K and (b) 298 K up to 1 bar. The CO_2 and N_2 sorption data weren't satisfied for the fitted parameters for COP-98B at 273 and 298 K.

very low. These results evidently recommend the importance of CO₂-philic functionality within the sorbent materials rather than exceptionally high surface areas—higher surface area is clearly not the imperative parameter for higher CO₂ capture capacity.

Since the CO₂ capture capacity and CO₂/N₂ selectivity should be governing factors for post-combustion CO₂ capture capacity, we studied COP-97B for regeneration under continuous flow of mixed gas experiments. The stability of CO₂ sorbent materials under repetitive cycles of CO₂ adsorption–desorption was examined in static conditions for COP-97B up to 10 cycles at 273 K (Fig. 5a). COP-97B was subjected to regeneration after each cycle at 80 °C under vacuum for 2 hours. CO₂ adsorption–desorption cycles show no loss of CO₂ capture efficiency and COP-97B demonstrated an average CO₂ capture capacity of 100 mg g⁻¹ (10% wt). The heat of adsorption for CO₂ adsorption in COP-97B is 46 kJ mol⁻¹, which facilitates desorption at quite a low temperature (80 °C) compared to the high temperatures (>120 °C) used in traditional aqueous amine scrubbing technology.

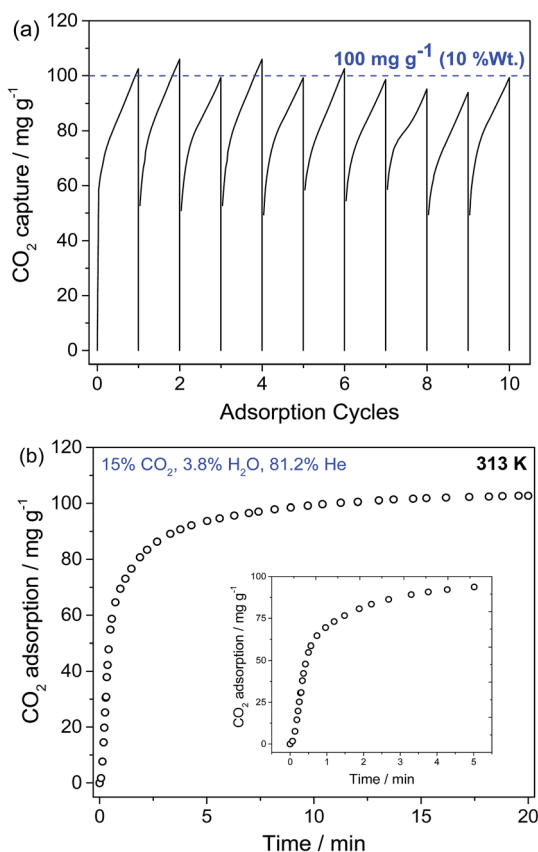


Fig. 5 (a) CO₂ adsorption cycles of COP-97B in static conditions at 273 K up to 1 bar. Desorption was carried out at 80 °C under vacuum for 2 hours. (b) CO₂ sorption of COP-97B for a 15% CO₂, 3.8% H₂O, 81.2% He gas mixture under flow conditions at 313 K up to 20 min. The gas mixture flow rate was 80 mL min⁻¹.

high CO₂ adsorptive materials. In summary, we developed and optimized, a commercially viable CO₂ sorbent by combining a wealth of knowledge set forth by the leaders in the field and our own design principles. Future studies will include the continuous development of low cost, robust porous COPs with a higher pore size (20–50 nm) to increase amine loading and thus even higher CO₂ capture capacities.

Acknowledgements

We acknowledge the financial support by grants from Korea CCS R&D Centre, Basic Science Research Program through the National Research Foundation of Korea (NRF) funded by the Ministry of Science, ICT & Future Planning (2013R1A1A1012998), IWT (NRF-2012-C1AAA001-M1A2A2026588), and KAIST EEWS Initiative.

Notes and references

- 1 C. Mora, A. G. Frazier, R. J. Longman, R. S. Dacks, M. M. Walton, E. J. Tong, J. J. Sanchez, L. R. Kaiser, Y. O. Stender, J. M. Anderson, C. M. Ambrosino, I. Fernandez-Silva, L. M. Giuseffi and T. W. Giambelluca, *Nature*, 2013, **502**, 183–187.
- 2 J. G. Canadell, C. Le Quere, M. R. Raupach, C. B. Field, E. T. Buitenhuis, P. Ciais, T. J. Conway, N. P. Gillett, R. A. Houghton and G. Marland, *Proc. Natl. Acad. Sci. U. S. A.*, 2007, **104**, 18866–18870.
- 3 J. Y. Wang, L. Huang, R. Y. Yang, Z. Zhang, J. W. Wu, Y. S. Gao, Q. Wang, D. O'Hare and Z. Y. Zhong, *Energy Environ. Sci.*, 2014, **7**, 3478–3518.
- 4 M. E. Boot-Handford, J. C. Abanades, E. J. Anthony, M. J. Blunt, S. Brandani, N. Mac Dowell, J. R. Fernandez, M. C. Ferrari, R. Gross, J. P. Hallett, R. S. Haszeldine, P. Heptonstall, A. Lyngfelt, Z. Makuch, E. Mangano, R. T. J. Porter, M. Pourkashanian, G. T. Rochelle, N. Shah, J. G. Yao and P. S. Fennell, *Energy Environ. Sci.*, 2014, **7**, 130–189.
- 5 S. Tedds, A. Walton, D. P. Broom and D. Book, *Faraday Discuss.*, 2011, **151**, 75–94.
- 6 Z. J. Zhang, Z. Z. Yao, S. C. Xiang and B. L. Chen, *Energy Environ. Sci.*, 2014, **7**, 2868–2899.
- 7 H. A. Patel, F. Karadas, A. Canlier, J. Park, E. Deniz, Y. Jung, M. Atilhan and C. T. Yavuz, *J. Mater. Chem.*, 2012, **22**, 8431–8437.
- 8 M. Sevilla, C. Falco, M. M. Titirici and A. B. Fuertes, *RSC Adv.*, 2012, **2**, 12792–12797.
- 9 H. Zhang, A. Goepfert, M. Czaun, G. K. S. Prakash and G. A. Olah, *RSC Adv.*, 2014, **4**, 19403–19417.
- 10 J. J. Vericella, S. E. Baker, J. K. Stolaroff, E. B. Duoss, J. O. Hardin, J. Lewicki, E. Glogowski, W. C. Floyd, C. A. Valdez, W. L. Smith, J. H. Satcher, W. L. Bourcier, C. M. Spadaccini, J. A. Lewis and R. D. Aines, *Nat. Commun.*, 2015, **6**, 6124.
- 11 M. B. Yue, Y. Chun, Y. Cao, X. Dong and J. H. Zhu, *Adv. Funct. Mater.*, 2006, **16**, 1717–1722.
- 12 W. G. Lu, M. Bosch, D. Q. Yuan and H. C. Zhou, *ChemSusChem*, 2015, **8**, 433–438.

- 13 C. Chen, S. T. Yang, W. S. Ahn and R. Ryoo, *Chem. Commun.*, 2009, 3627–3629, DOI: 10.1039/b905589d.
- 14 C. Chen, J. Kim and W. S. Ahn, *Korean J. Chem. Eng.*, 2014, **31**, 1919–1934.
- 15 A. Goepfert, H. Zhang, M. Czaun, R. B. May, G. K. S. Prakash, G. A. Olah and S. R. Narayanan, *ChemSusChem*, 2014, **7**, 1386–1397.
- 16 M. G. Schwab, B. Fassbender, H. W. Spiess, A. Thomas, X. L. Feng and K. Mullen, *J. Am. Chem. Soc.*, 2009, **131**, 7216–7217.
- 17 J. Byun, S. H. Je, H. A. Patel, A. Coskun and C. T. Yavuz, *J. Mater. Chem. A*, 2014, **2**, 12507–12512.
- 18 A. Sayari, A. Heydari-Gorji and Y. Yang, *J. Am. Chem. Soc.*, 2012, **134**, 13834–13842.
- 19 A. Goepfert, M. Czaun, R. B. May, G. K. S. Prakash, G. A. Olah and S. R. Narayanan, *J. Am. Chem. Soc.*, 2011, **133**, 20164–20167.
- 20 H. A. Patel, S. H. Je, J. Park, Y. Jung, A. Coskun and C. T. Yavuz, *Chem.–Eur. J.*, 2014, **20**, 772–780.
- 21 H. A. Patel, S. H. Je, J. Park, D. P. Chen, Y. Jung, C. T. Yavuz and A. Coskun, *Nat. Commun.*, 2013, **4**, 1357.
- 22 G. G. Qi, L. L. Fu, B. H. Choi and E. P. Giannelis, *Energy Environ. Sci.*, 2012, **5**, 7368–7375.
- 23 Z. H. Chen, S. B. Deng, H. R. Wei, B. Wang, J. Huang and G. Yu, *ACS Appl. Mater. Interfaces*, 2013, **5**, 6937–6945.
- 24 A. Goepfert, S. Meth, G. K. S. Prakash and G. A. Olah, *Energy Environ. Sci.*, 2010, **3**, 1949–1960.